Analytica Chimica Acta 724 (2012) 111–118

Contents lists available at SciVerse ScienceDirect

Analytica Chimica Acta

journal homepage: www.elsevier.com/locate/aca

Sequential-dissociation kinetics of non-covalent complexes of DNA with multiple proteins in separation-based approach: General theory and its application

Leonid T. Cherney, Victor Okhonin, Alexander P. Petrov, Sergey N. Krylov*

Department of Chemistry and Centre for Research on Biomolecular Interactions, York University, Toronto, Ontario M3J 1P3, Canada

ARTICLE INFO

Article history:
Received 28 October 2011
Received in revised form 27 January 2012
Accepted 29 January 2012
Available online 19 February 2012

Keywords:
Protein–DNA interaction
Protein machines
Kinetics
Capillary electrophoresis

ABSTRACT

Binding of multiple proteins to DNA is crucial in many regulatory cellular processes. The kinetics of assembly and disassembly of DNA–multiple protein complexes is very difficult to study in detail due to the lack of suitable experimental approaches. A separation-based approach has been recently proposed to resolve disassembly kinetics of such complexes. While conceptually simple, the separation-based approach generates experimental data with very complex patterns. The analysis of these patterns is a challenging problem on its own. Here we report on a mathematical approach that can extract a solution for the experimental data obtained in separation-based analysis of sequential dissociation of a DNA complex with multiple proteins. This case describes the dissociation of proteins one-by-one from the complex. Generally speaking, a mathematical solution of such problems requires calculations of multiple integrals. Our approach reduces this procedure to taking double integrals and constructing their superposition. We tested this approach with the experimental data obtained for three-step sequential dissociation of complexes of DNA with two protein copies.

1. Introduction

Binding of multiple proteins to a single DNA molecule is common in cell biology and plays a key role in regulation of gene expression, DNA replication, DNA integrity control, and viral replication [1,2]. Understanding the dynamics of these fundamental biological processes often requires knowledge of the kinetic and thermodynamic parameters for each individual step of formation and dissociation of the relevant complexes between multiple proteins and DNA [3–5]. In these complexes, proteins can be bound to the DNA directly or indirectly through other proteins. Typically, the knowledge of complexes of multiple proteins with DNA does not exceed the identities of the interacting proteins and DNA [6]. Some information on kinetics and thermodynamics can be obtained with conventional experimental methods such as surface plasmon resonance (SPR) [7,8], microcalorimetry [9], gel electrophoresis [10], analytical ultracentrifugation [11,12], stopped flow technique [13,14], and affinity capillary electrophoresis (ACE) [15–18]. The applicability of these methods to kinetic studies on the formation and dissociation of DNA–multiple protein complexes can be limited due to the difficulties of distinguishing kinetics of multiple interconnected processes. Such distinction is especially difficult when the rates of the processes are of the same order of magnitude [19,20].

Kinetic capillary electrophoresis (KCE) methods use a separation-based approach for studying kinetics and thermodynamics of non-covalent complexes of biological molecules [21–28]. We recently implemented a similar approach for the analysis of dissociation kinetics of DNA complexed with multiple proteins [29]. The approach is based on our general understanding that the kinetics of all processes that occur during the formation and/or dissociation of DNA–multiple proteins complexes can be easier distinguished if different complexes move with different velocities, or, in other words, are spatially separated. As a practical means of introducing differential mobilities of different DNA–protein complexes we used capillary electrophoresis (CE) [23]. CE simply provides an efficient way to accomplish the separation-based analysis of simultaneous dissociation processes involving DNA–multiple protein complexes. The resultant experimental data encompass a complex interplay of mass transfer with dissociation kinetics; the analysis of such data is a significant challenge. While such data can always be analyzed numerically, the numerical approaches often lack the transparency in problems with a large number of parameters that have to be determined. In contrast, analytical solutions are often more transparent and allow general conclusions to be drawn. Therefore, it is important to find exact mathematical solutions that can be used to analyze data obtained through separation based dissociation of multiple proteins bound to DNA. Here we describe the analytical solution for the separation-based kinetic analysis of multi-step sequential

Abbreviations: CE, capillary electrophoresis; SPR, surface plasmon resonance; SSB, single strand DNA binding.

* Corresponding author. Tel.: +1 416 7362100x22345; fax: +1 416 736 5936.
E-mail address: skrylov@yorku.ca (S.N. Krylov).

0003-2670/$ – see front matter © 2012 Elsevier B.V. All rights reserved.
doi:10.1016/j.aca.2012.01.057

dissociation of DNA–multiple protein complexes. A straightforward solution for N dissociation steps would require taking an integral of the Nth order, which is not feasible for large N. We propose a reduction approach that presents the solution as a superposition of N integrals of the second order, which is always feasible. We tested our approach with experimental data obtained from the three-step sequential dissociation of DNA–protein complexes with two protein copies. The further progress in separation-based kinetic analysis of DNA–multiple protein complexes depends on inventiveness in the development of practical mathematical tools for data analysis.

2. Results and discussion

2.1. Basic equations of sequential-dissociation kinetics

In general, to study the sequential dissociation kinetics of DNA–multiple protein complexes the following two-step operation should be performed. In step 1, N DNA–protein complexes (C_1, …, C_N) are formed by incubating free DNA (C_0) with protein (P), long enough to ensure each binding reaction approaches equilibrium:

$$\begin{aligned} &C_0 \overset{P,K_{d,1}}{\rightleftarrows} C_1 \overset{P,K_{d,2}}{\rightleftarrows} C_2 \cdots \overset{P,K_{d,N}}{\rightleftarrows} C_N \\ &C_0 \equiv D, \quad C_1 \equiv DP, \quad C_2 \equiv DPP, \quad \ldots, \quad C_N \equiv D\underbrace{P\cdots P}_{N} \end{aligned} \tag{1a}$$

In reaction (1a), $K_{d,1}, K_{d,2}, \ldots, K_{d,N}$ are equilibrium dissociation constants of N sequential reactions. DNA is assumed to have enough binding sites for multiple protein molecules. In the second step, unbound proteins are continuously removed from the complexes so that the rates of the forward processes in reaction (1a) become zero and the complexes are forced to dissociate:

$$C_N \xrightarrow{k_N} C_{N-1} \xrightarrow{k_{N-1}} C_{N-2} \xrightarrow{k_{N-2}} \cdots \xrightarrow{k_1} C_0 \tag{2}$$

where k_N, k_{N-1}, …, k_1 in reaction (2) are the dissociation rate constants for N DNA–protein complexes. In the separation-based approach, all complexes and unbound DNA should undergo continuous separation in this step, resulting in spatial segregation of the dissociation kinetics (hereafter DNA is also referred to as "complex" C_0 that contains zero proteins). The described operation can also be applied to protein–DNA complexes involving several different proteins if such complexes dissociate consequently, as shown in (2). In this case, reaction (1a) should be rewritten as follows:

$$\begin{aligned} &C_0 \overset{P_1,K_{d,1}}{\rightleftarrows} C_1 \overset{P_2,K_{d,2}}{\rightleftarrows} C_2 \cdots \overset{P_N,K_{d,N}}{\rightleftarrows} C_N \\ &C_0 \equiv D, \quad C_1 \equiv DP_1, \quad C_2 \equiv DP_1P_2, \quad \ldots, \quad C_N \equiv DP_1\cdots P_N \end{aligned} \tag{1b}$$

where proteins are numbered (with subscripts 1, 2, …, N) according to the order of protein association during formation of complexes. Thus, in theory, all proteins may be different. Furthermore, the separation-based approach works in the presence of conformational changes in protein–DNA complexes if such transformations can occur only consequently, after the separation of complexes. For example, in the case of a conformational change in the complex with only one protein, reaction (1a) should be modified as follows:

$$\begin{aligned} &C_0 \overset{P,K_{d,1}}{\rightleftarrows} C_1 \overset{K_{d,2}}{\rightleftarrows} C_2 \overset{P,K_{d,3}}{\rightleftarrows} C_3 \cdots \overset{P,K_{d,N}}{\rightleftarrows} C_N \\ &C_0 \equiv D, \quad C_1 \equiv (DP)^a, \quad C_2 \equiv (DP)^b, \quad C_3 \equiv DPP, \quad \ldots, \quad C_N \equiv D\underbrace{P\cdots P}_{N-1} \end{aligned} \tag{1c}$$

Here, protein–DNA complexes in two conformations, a and b, are numbered according to the transition between them in sequential reactions (2). In this case, subscript $n = 1, 2, \ldots, N$ denotes a serial number of complex C_n in sequential dissociation (2) (in the reverse order) and may not coincide with the number of proteins bound to DNA in complex C_n. All results obtained below are applicable to reactions (1a)–(1c) as long as mainly sequential reactions (2) take place after removing the unbound protein from the complexes.

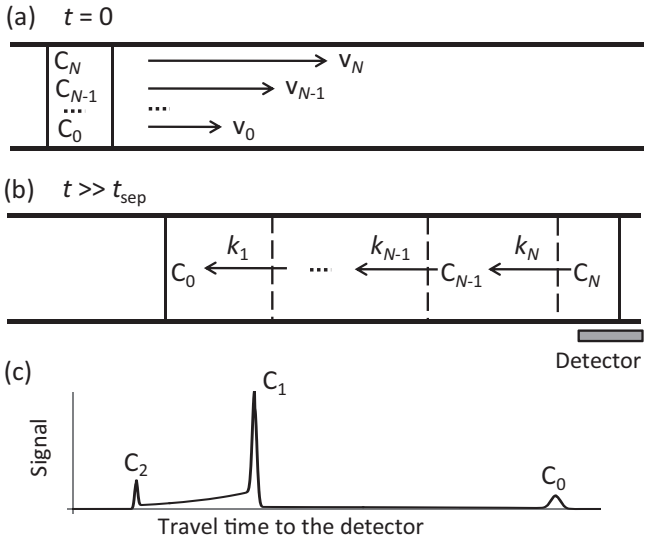

Fig. 1. Schematic illustration of the separation-based approach for studying sequential dissociation of complexes C_N, C_{N-1}, …, C_1 formed by DNA (C_0) and multiple proteins. (a) The initial mixture of complexes introduced at $t = 0$ (the plug is shown between two vertical lines). (b) Separation of complexes at $t \gg t_{sep,n} \sim W/\Delta v_n$ ($n = 1$, …, N) where W is the initial plug length and $\Delta v_n = |v_n - v_{n-1}|$ is the difference between velocities of complexes that are "neighbors" in the sequential dissociation (2). Dashed lines denote approximate boundaries between the complexes. A cumulative signal from all complexes and DNA is measured by a detector. (c) A typical signal from the mixture of DNA and two complexes when most of DNA in the initial plug is bound to proteins.

Many other processes can be described by models similar to (2) [30,31].

The implementation of our method using CE can be described as follows. In step 1, the equilibrium mixture of the complexes (see reactions (1a)–(1c)) is prepared in solution and a short plug of it is introduced into a narrow and long capillary that is coaxial with the x coordinate (Fig. 1a). The velocities $v_0, v_1, \ldots$ and v_N and initial concentrations of each component does not change significantly across the capillary. The longitudinal Peclet number is very large. Such a reactor can usually be considered as a one-dimensional infinite reactor, in which longitudinal diffusion is negligible. In step 2, complexes C_0, C_1, … and C_N are continuously separated from unbound proteins and each other by moving with different velocities (Fig. 1b). The dissociation kinetics of individual complexes are spatially separated and cumulative signal acquires $N + 1$ peaks corresponding to complexes $C_0, C_1, \ldots$ and C_N that were present in the initial mixture. Fig. 1c shows a typical electropherogram for a mixture of C_0, C_1, and C_2 ($N = 2$) with two-step sequential dissociation.

Since the rates of the forward processes in reaction (2) are negligible, the multistage dissociation of each and every complex in the initial equilibrium mixture defined by equation (1a) (or (1b) and (1c)) can be considered independent of the dissociation of all other complexes. As a result, kinetics of multistage dissociation of complexes, starting from any complex n in the initial mixture ($0 \le n \le N$) and continuing to complex 0, can be described by the following system of $n + 1$ partial differential equations:

$$(\partial_t + v_n\partial_x + k_n)C_n^n(x,t) = A_n^0\delta(x)\delta(t) \quad (n = N, \ldots, 0; k_0 = 0) \tag{3}$$

$$(\partial_t + v_q\partial_x + k_q)C_q^n(x,t) = k_{q+1}C_{q+1}^n(x,t) \quad (q = n-1, \ldots, 0; n > 0) \tag{4}$$

Here, A_n^0 is the total amount of the initial complex n added at $t=0$, C_n^n is the current linear concentration of the initial complex n, C_q^n (at $q<n$) is the linear concentration of a part of complex C_q that formed as a result of dissociation started from the initial complex C_n, v_j and $k_j \equiv k_{off,j}$ are the velocity and the dissociation rate constant of complex j ($0 \le j \le n$). Linear concentrations of the complexes are defined as their amounts per unit length of the capillary. At $n=0$, equation (3) describes the propagation of free DNA ("complex" C_0). Concentrations of complexes present in (3) and (4) depend on the distance from the point where separation started, x, and on the time interval, t, passed from the beginning of separation. In (3), we use Dirac's δ-functions to define distributions of initial complexes in the sample plug. This approach allows us to simplify mathematical transformations in the process of solving equations (3) and (4). In the final solution, these functions should be approximated by using normal distributions. It is also assumed that before $t=0$, all concentrations are equal to zero, and that the modeled system has an infinite length in both directions, so that there is no influence from boundaries.

Finally, the multistage dissociation of whole initial mixture (1a) (or (1b) and (1c)) is described by equations (3) and (4) at all possible values of n. This corresponds to the superposition of dissociation processes that start with each complex in the initial mixture. As a result, the total concentration C_q of any complex q is determined through the summation of its concentrations resulting from the dissociation of all complexes present in the initial mixture:

$$C_q(x,t) = \sum_{n=q}^{N} C_q^n(x,t) \quad (q = N, \ldots, 0) \tag{5}$$

Relations (3)–(5) contain concentrations of complexes whereas the experimental data, such as electropherograms, operate with signals (optical, electrochemical, etc.). The signal S_q generated by the complex q is usually proportional to its total concentration C_q. As a result, we have

$$S_q(x,t) = g_q C_q(x,t), \qquad S(x,t) \equiv \sum_{q=0}^{N} S_q = \sum_{q=0}^{N} g_q C_q(x,t) \tag{6}$$

where S is a total signal generated by all complexes and free DNA. Coefficients g_q can be different and are determined by the nature of signals used to detect complexes. The rate constants of dissociation can be determined by fitting the total experimental signal with a curve $S(t)$ found from (6) at a value of x corresponding to the detector's position. To do this, one needs to know functions $C_q(x,t)$ which can be expressed in terms of $C_q^n(x,t)$ according to relations (5).

2.2. Analytical solutions for concentrations of complexes

The major goal of this work was to find an analytical solution for system (3) and (4) which is $n+1$ dependencies of the concentrations, C_q^n, on time, spatial coordinate, as well as velocities, v_j, and dissociation rate constants, k_j, of corresponding complexes: $C_q^n(x,t,k_q,\ldots,k_n,v_q,\ldots,v_n)$ where $q=n, \ldots, 0$. One of the ways to solve the system of equations (3) and (4) is to obtain the right-hand side of the equation for concentration of each complex with number q by integrating the concentration equation for the corresponding complex with number $q+1$. In this way, expressions describing concentrations of later (in sequence (2)) complexes will be high order multiple integrals; they would be very difficult to solve directly. Here, we explain a simpler alternative, which can calculate the concentrations of later complexes without the need of computing multiple integrals. In essence, we found a way of solving the system of equations (3) and (4) which requires computing only double integrals. This approach leads to expressions for C_q^n which are linear superpositions of double integrals that, in turn, can be easily calculated.

By using the Fourier transform:

$$C_q^n = \frac{1}{2\pi} \int \hat{C}_q^n(\omega,\zeta) e^{i(\omega t + \zeta x)} d\omega d\zeta, \quad q \le n \tag{7}$$

differential equations (3) and (4) can be reduced to the following linear algebraic equations:

$$d_n \hat{C}_n^n(x,t) = (2\pi)^{-1} A_n^0, \qquad d_q \hat{C}_q^n(x,t) = k_{q+1} \hat{C}_{q+1}^n \quad (q < n) \tag{8}$$

where

$$d_q \equiv i\omega + i v_q \zeta + k_q \quad (q \le n) \tag{9}$$

Solution to (8) has a form

$$\hat{C}_n^n = \frac{A_n^0}{2\pi d_n}; \qquad \hat{C}_q^n = \frac{A_n^0}{2\pi} \prod_{r=q+1}^{n} k_r \prod_{j=q}^{n} \frac{1}{d_j}, \quad (q < n) \tag{10}$$

The calculation of integral in (7) at $q=n$ gives:

$$C_n^n(x,t) = A_n^0 \delta(x - v_n t) \exp(-k_n t) \theta(t) \tag{11}$$

where $\theta(t)$ is the θ-function ($\theta(t)=1$ at $t \ge 0$ and $\theta(t)=0$ at $t<0$). Direct substitution of (11) into the first equation in (3) also shows that (11) is a solution of this equation. To find C_q^n at $q<n$, it is useful to present the product in expression (10) for C_q^n in the form:

$$\prod_{j=q}^{n} \frac{1}{d_j} = \sum_{n \ge j > p \ge q} \frac{Q_{jp}^{nq}}{d_j d_p} \quad (q < n), \tag{12}$$

where the sum is taken over all pairs of indexes (j, p) that satisfy condition $n \ge j > p \ge q$. Coefficients Q_{jp}^{nq} must satisfy the following equations:

$$\sum_{n \ge j > p \ge q} \left(Q_{jp}^{nq} \prod_{s=q; s \ne j,p}^{n} d_s \right) = 1 \quad (q < n) \tag{13}$$

for relation (12) to be valid. The product in (13) does not contain multipliers d_j and d_p. Conditions (13) can be easily obtained from (12) by multiplying its both sides by $d_q d_{q+1} \ldots d_n$. Since quantities d_s depend on independent variables ζ and ω, the left-hand side of (13) is a polynomial with respect to variables ζ and ω. Its terms are proportional to products $\zeta^a \omega^b$. Powers a and b (should not be confused with the DP conformations in reaction (1c)) satisfy a condition $0 \le a+b \le n-q-1$ that follows from (9) and (13). Coefficients at products $\zeta^a \omega^b$ in this polynomial can be expressed in terms of sums of various products of v_q, k_q, and Q_{jp}^{nq}. Obviously, equations (13) can be satisfied only if coefficients at all products $\zeta^a \omega^b$ are the same at both sides of (13). As a result, we have obtained the following linear algebraic equations which determine Q_{jp}^{nq}:

$$\sum_{n \ge j > p \ge q} (Q_{jp}^{nq} V_{jp}^{anq} K_{jp}^{bnq}) = \delta_{a,0} \delta_{b,n-q-1} \quad q < n, \quad 0 \le a+b \le n-q-1 \tag{14}$$

$$V_{jp}^{anq} = \sum_{r_1, r_2 \cdots r_a \ne j,p} v_{r_1} v_{r_2} \cdots v_{r_a} \quad \text{at} \quad a > 0 \qquad q \le r_1 < r_2 < \cdots < r_a \le n, \quad V_{jp}^{anq} = 0 \quad \text{at} \quad a = 0 \tag{15}$$

$$K_{jp}^{bnq} = \sum_{s_1, s_2 \cdots s_b \ne j,p} k_{s_1} k_{s_2} \cdots k_{s_b}, \quad \text{at} \quad b > 0 \qquad q \le s_1 < s_2 < \cdots < s_b \le n, \quad K_{jp}^{bnq} = 0 \quad \text{at} \quad b = 0 \tag{16}$$

Here a and b are indexes rather than powers. For each fixed pair of indexes nq, the number L_{nq} of unknown coefficients Q_{jp}^{nq}

$(n \geq j > p \geq q)$ coincides with the number of equations in (14) and is determined by the following relation:

$$L_{nq} = 1 + 2 + \cdots + (n-q) = \frac{1}{2}(n-q+1)(n-q) \quad (q < n < N) \quad (17)$$

As a result, the expression for C_q^n at $q < n$ can be presented in the following form:

$$C_q^n(x,t) = A_n^0 \prod_{r=q+1}^{n} k_r \sum_{n \geq j > p \geq q} Q_{jp}^{nq} G_{jp} \quad (q < n) \quad (18)$$

$$G_{jp}(x,t) = \frac{1}{(2\pi)^2} \iint \frac{e^{i(\omega t + \varsigma x)} d\omega d\varsigma}{d_j d_p} \quad (19)$$

Functions $G_{jp}(x,t)$ satisfy a simple equation:

$$(\partial_t + v_j \partial_x + k_j)(\partial_t + v_p \partial_x + k_p) G_{jp}(x,t) = \delta(x)\delta(t) \quad (20)$$

They are determined by expression:

$$G_{jp}(x,t) = \frac{1}{|v_p - v_j|} \theta\left(\frac{X_j}{v_p - v_j}\right) \theta\left(\frac{X_p}{v_j - v_p}\right) \exp\left(\frac{k_j X_p - k_p X_j}{v_p - v_j}\right) \quad (21)$$

where $X_s \equiv x - v_s t$ ($s = j, p$) and θ is the θ-function.

Thus, a general solution of equations (3) and (4) governing multistage dissociation of complexes is given by relation (11) for $C_n^n(x,t)$ and by expressions (18) and (21) for $C_q^n(x,t)$ at $q < n$. Unknown quantities Q_{jp}^{nq} can be found from the system of linear algebraic equations (14) if:

$$\det ||V_{jp}^{anq} K_{jp}^{bnq}|| \neq 0 \quad (22)$$

for each pair of indexes nq. Here, det denotes the determinant of system (14) calculated at fixed values of indexes nq. Pairs of indexes ab and jp denote, respectively, rows and columns of matrix in (22). The determinant value depends on arguments listed in (22). Conditions (22) are usually satisfied since the opposite case where det = 0 means that some relations between velocities and dissociation rate constants should take place. For example, such a relation would require an exact proportionality between the dissociation rate constants and the velocity differences in the case of $n = 2$ (see equation (31) in the next subsection):

$$k_1 = \chi(v_1 - v_0), \qquad k_2 = \chi(v_2 - v_0) \quad (23)$$

where χ is an arbitrary constant. Obviously, conditions similar to (23) cannot be satisfied rigorously due to the approximate nature of velocities and dissociation rate constants. Nevertheless, such special cases need additional consideration. In particular, if the parameters are approximately satisfy the relation det = 0, the accuracy of the present approach can be affected.

According to expressions (18) which describe an arbitrary multistage dissociation (2), the corresponding mathematical solution can be expressed as a linear superposition of all terms G_{jp} associated with the following type of processes:

$$C_j \xrightarrow{k_j} C_p \xrightarrow{k_p} \quad (24)$$

A single term, G_{jp}, determined by (21) includes only four parameters: v_j, v_p, k_j, and k_p. In essence, any multistage dissociation can be presented as a linear superposition of one or more dissociations of the type depicted by (24). The formal dissociation in (24) can include real processes (e.g. $C_{n-1} \rightarrow C_{n-2}$) and virtual processes (e.g. $C_{n-1} \rightarrow C_{n-3}$) that are not experimentally feasible. Our linear superposition approach allows us to significantly simplify solutions of equations for the multistage dissociation of complexes with different stoichiometries.

It is worth noting that equations (3) and (4) will describe any sequential reactions of the type (2) if the latter can be considered as reactions of the first order. Obvious examples include sequential conformation change of components C_N, C_{N-1}, …, C_1 or their sequential association with another component (for example, ligand) that is present in a significant excess relative to C_N, C_{N-1}, …, C_1. In such cases, the obtained analytical solutions of equations (3) and (4) can be used to find concentrations of all components in (2).

2.3. Simplified solutions for two- and three-stage reactions

We consider the application of the developed generalized theory to the first three stages of the multi-stage sequential dissociation of complexes (including possible conformation changes) as follows:

$$C_n \xrightarrow{k_n} C_{n-1} \xrightarrow{k_{n-1}} C_{n-2} \xrightarrow{k_{n-2}} C_{n-3} \xrightarrow{k_{n-3}} \cdots \quad (25)$$

Dissociation (25) has n stages (since $k_0 = 0$) and can start from any complex C_n present in the initial mixture. If $n = 0$, sequence (25) has only one term C_0 and no dissociation stages. At all n ($0 \leq n \leq N$) concentration C_n^n of the complex C_n itself is given by (11).

If $n \geq 1$, there is the second complex C_{n-1} in (25) and its concentration C_{n-1}^n is determined by relations (18) at $q = n - 1$:

$$C_{n-1}^n(x,t) = A_n^0 k_n Q_{n,n-1}^{n,n-1} G_{n,n-1} = A_n^0 k_n G_{n,n-1} \quad (Q_{n,n-1}^{n,n-1} = 1) \quad (26)$$

Here we took into account that equations (14) give $Q_{n,n-1}^{n,n-1} = 1$ for $q = n - 1$.

If $n \geq 2$, there is the third complex C_{n-2} in (25) and its concentration, C_{n-2}^n, is determined by relations (18) at $q = n - 2$:

$$C_{n-2}^n(x,t) = A_n^0 k_n k_{n-1} \times (Q_{n,n-1}^{n,n-2} G_{n,n-1} + Q_{n,n-2}^{n,n-2} G_{n,n-2} + Q_{n-1,n-2}^{n,n-2} G_{n-1,n-2}) \quad (27)$$

In this case equations (14) reduce to the following system for the coefficients $Q_{n,n-1}^{n,n-2}$, $Q_{n,n-2}^{n,n-2}$, and $Q_{n-1,n-2}^{n,n-2}$

$$\begin{pmatrix} k_{n-2} & k_{n-1} & k_n \\ v_{n-2} & v_{n-1} & v_n \\ 1 & 1 & 1 \end{pmatrix} \begin{pmatrix} Q_{n,n-1}^{n,n-2} \\ Q_{n,n-2}^{n,n-2} \\ Q_{n-1,n-2}^{n,n-2} \end{pmatrix} = \begin{pmatrix} 1 \\ 0 \\ 0 \end{pmatrix} \quad (28)$$

Their solution is given by:

$$Q_{n,n-1}^{n,n-2} = \frac{v_{n-1} - v_n}{\det}, \qquad Q_{n,n-2}^{n,n-2} = \frac{v_n - v_{n-2}}{\det}, \qquad Q_{n-1,n-2}^{n,n-2} = \frac{v_{n-2} - v_{n-1}}{\det} \quad (29)$$

$$\det = (k_{n-1} - k_{n-2})(v_n - v_{n-2}) - (k_n - k_{n-2})(v_{n-1} - v_{n-2}) \quad (30)$$

At $n = 2$ the expression (30) becomes simpler since C_0 does not dissociate further and, therefore, $k_0 = 0$:

$$\det = k_1(v_2 - v_0) - k_2(v_1 - v_0) \quad (31)$$

Given (31), we see that condition det = 0 at $n = 2$ is equivalent to relations (23).

If $n \geq 3$ there is the forth complex C_{n-3} in (25) and its concentration C_{n-3}^n is determined by relations (18) at $q = n - 3$:

$$C_{n-3}^n(x,t) = A_n^0 k_n k_{n-1} k_{n-2} \times (Q_{n,n-1}^{n,n-3} G_{n,n-1} + Q_{n,n-2}^{n,n-3} G_{n,n-2} + Q_{n-1,n-2}^{n,n-3} G_{n-1,n-2} + Q_{n,n-3}^{n,n-3} G_{n,n-3} + Q_{n-1,n-3}^{n,n-3} G_{n-1,n-3} + Q_{n-2,n-3}^{n,n-3} G_{n-2,n-3}) \quad (32)$$

Now equations (14) can be presented as the following linear algebraic system of the sixth order:

$$\begin{pmatrix} 1 & 1 & 1 & 1 & 1 & 1 \\ \nu_{n-2}+\nu_{n-3} & \nu_{n-1}+\nu_{n-3} & \nu_n+\nu_{n-3} & \nu_{n-1}+\nu_{n-2} & \nu_n+\nu_{n-2} & \nu_n+\nu_{n-1} \\ \nu_{n-2}\nu_{n-3} & \nu_{n-1}\nu_{n-3} & \nu_n\nu_{n-3} & \nu_{n-1}\nu_{n-2} & \nu_n\nu_{n-2} & \nu_n\nu_{n-1} \\ k_{n-2}+k_{n-3} & k_{n-1}+k_{n-3} & k_n+k_{n-3} & k_{n-1}+k_{n-2} & k_n+k_{n-2} & k_n+k_{n-1} \\ \nu_{(n-2}k_{n-3)} & \nu_{(n-1}k_{n-3)} & \nu_{(n}k_{n-3)} & \nu_{(n-1}k_{n-2)} & \nu_{(n}k_{n-2)} & \nu_{(n}k_{n-1)} \\ k_{n-2}k_{n-3} & k_{n-1}k_{n-3} & k_nk_{n-3} & k_{n-1}k_{n-2} & k_nk_{n-2} & k_nk_{n-1} \end{pmatrix} \begin{pmatrix} Q_{n,n-1}^{n,n-3} \\ Q_{n,n-3}^{n,n-3} \\ Q_{n,n-2}^{n,n-3} \\ Q_{n-1,n-2}^{n,n-3} \\ Q_{n,n-3}^{n,n-3} \\ Q_{n-1,n-3}^{n,n-3} \\ Q_{n-2,n-3}^{n,n-3} \end{pmatrix} = \begin{pmatrix} 0 \\ 0 \\ 0 \\ 0 \\ 0 \\ 1 \end{pmatrix} \tag{33}$$

where we used a notation $\nu_{(A}k_{B)} = \nu_A k_B + \nu_B k_A$. At $n = 3$ equations (33) become simpler since the terms with k_0 vanish. An explicit solution for (33) is too cumbersome and it is easier to numerically find coefficients $Q_{jp}^{n,n-3}$ $(n \geq j > p \geq n-3)$ directly from (33). In the case of two- and three-stage dissociation kinetics ($N = 2$ and 3), relations (11), (21), and (26)–(33) allow one to calculate all terms C_q^n present in expression (5) for the total concentration of each complex. After that, the cumulative signal can be determined by using expression (6) with values for coefficients g_q measured experimentally. These calculations require velocities ν_n, the rate constants k_n, and the total amounts A_n^0 of all complexes in the initial mixture to be known. Usually, this is not the case in studying sequential dissociation kinetics. Alternatively, these parameters can be determined to satisfy the condition of the best fit between the theoretical signal and the one measured experimentally.

2.4. Examples of method application to experimental data analysis

Let us test the developed theory by applying it to the study of dissociation kinetics of complexes formed by a 79-nt long single stranded DNA and single-strand DNA binding (SSB) protein from *Escherichia coli*. This SSB protein plays an important role in DNA replication, recombination, and repair and has been studied extensively by both pure biochemical and crystallographic methods [32–40].

Fig. 2 demonstrates signals with four peaks that can be assigned to free DNA ($C_0 \equiv D$) and three complexes ($C_1 \equiv (DP)^a$, $C_2 \equiv (DP)^b$, and $C_3 \equiv DPP$) that were present in the initial mixture. Such assignments of peaks in Fig. 2 are based on the following considerations. First of all, the migration time of pure DNA (C_0) is known from a CE run of DNA only, which allows us to assign the slowest peak to DNA. The 79-nt single-stranded DNA can bind a maximum of two tetramers of SSB protein. When a single protein is bound, two binding modes with different DNA conformations are possible under the same experimental conditions [34]. These modes differ in the number of protein-bound nucleotides; the more nucleotides bound, the more restricted the conformation of DNA. Finally, the DNA–protein complex should move to the detector faster when the number of bound proteins increases. Indeed, a negatively charged complex with a larger number of proteins has a smaller electrophoretic mobility and, therefore, is slowed down to a lesser

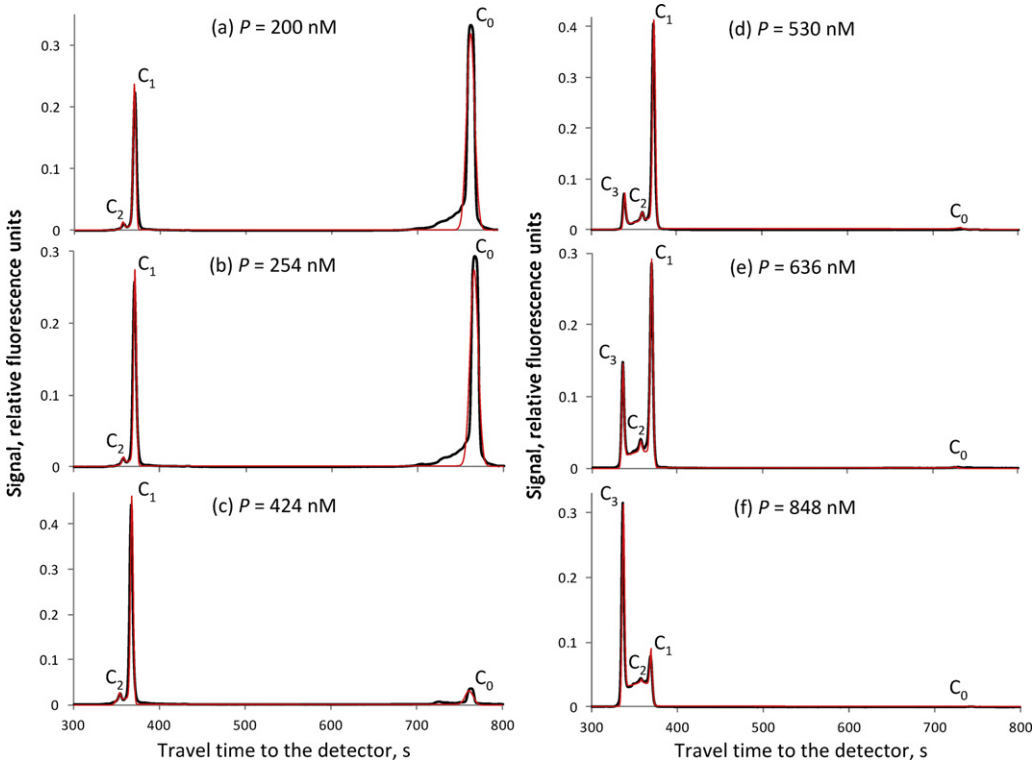

Fig. 2. Experimental (black line) and theoretical (red line) signals for three-stage dissociation kinetics ($N = 3$). The theoretical curves correspond to the best-fit model with relative errors of less than 5.6%. The experimental curves are obtained for mixtures of a 79-nt long single stranded DNA and a single-strand DNA binding (SSB) protein from *E. coli*. Six mixtures of DNA and protein were used with varying concentrations P of the SSB protein (shown in the figure) and a single concentration of DNA ($D = 200$ nM) before the formation of complexes. The detector was placed at a distance of 40 cm from the initial plug. Peaks C_0, C_1, C_2, and C_3 correspond to D, $(DP)^a$, $(DP)^b$, and DPP, respectively. In panels (a)–(c), the peaks of C_3 are not detectable since the concentration of DPP in the initial plug is too small at lower values of P. DPP almost completely dissociated before it reached the detector. This dissociation resulted in the exponential-like curves to the left of the peaks of C_2. (For interpretation of the references to color in this figure legend, the reader is referred to the web version of the article.)

extent by an electric field that is directed to the detector along the electroosmotic flow. In Fig. 2, for example, $C_3 \equiv$ DPP moves faster and contains more proteins than $C_2 \equiv (DP)^b$ and $C_1 \equiv (DP)^a$. C_2 and C_1, in turn, move faster and contain more proteins than $C_0 \equiv$ D. Out of the two complexes with the same number of proteins (C_2 and C_1 in Fig. 2), the one with a more restricted conformation of DNA should have a smaller electrophoretic mobility and move to the detector faster than the one with a less restricted conformation. Therefore, C_2 corresponds to a more restricted DNA conformation with more nucleotides bound. Using these facts, one can easily determine the number of complexes that are present in the reaction mixture by qualitatively studying data in Fig. 2 and, therefore, determine the parameter N in model (1c).

Calculated theoretical signals for three-stage dissociation are depicted by red lines in Fig. 2. Again, the peaks correspond to the complexes that populate the initial mixture. The exponential-like curves between the peaks result from dissociation of these complexes. Table 1 shows the dissociation rate constants, k_C, of complexes $C = (DP)^a$, $(DP)^b$, and DPP found from the best fit procedure applied to data in Fig. 2. This table also contains the association rate constants, $k_{on,C}$, of complex C, the equilibrium dissociation constants, $K_{d,C}$, of complex C, and equilibrium concentrations D^0 and P^0 of free DNA and unbound SSB protein in the initial plug. The values of $K_{d,C}$, D^0, and P^0 were calculated using: (i) the initial equilibrium amounts, A_n^0, of complexes that were also determined from the best fit, (ii) a known total amount of free and bound DNA in the initial plug, (iii) a known total amount of free and bound protein in the initial plug, and (iv) the volume of the initial plug. Values of $k_{on,C}$ were obtained from the following relationship between the rate and equilibrium constants:

$$k_{on,C} = \frac{k_C}{K_{d,C}} \quad \text{where} \quad C = (DP)^a, (DP)^b, DPP \tag{34}$$

In almost all the cases, the rate constant for conformation change of $(DP)^b$ into $(DP)^a$ is significantly higher than that for the reverse reaction (Table 1) and, therefore, the latter can be neglected in calculations of the $(DP)^b$ concentration (except for $P = 848$ nM). Generally speaking, this reverse conformation change should be taken into account in calculations of the $(DP)^a$ concentration. However, the latter will not be affected significantly due to small values of corresponding rate constants.

The main purpose of experiments shown in Fig. 2 was to illustrate mathematical methods developed for studying sequential dissociation kinetics by the separation-based approach. Nevertheless, some important conclusions can be derived directly from these experiments even without the use of obtained analytical solutions of equations (3) and (4). These conclusions also allow one to check and confirm the developed mathematical methods.

Firstly, the increase in the concentration of SSB results in smaller DNA peaks and more prominent peaks denoted by $C_1 = (DP)^a$, $C_2 = (DP)^b$, and $C_3 =$ DPP in Fig. 2. Therefore, the peaks of C_1, C_2, and C_3 should, indeed, correspond to DNA–protein complexes.

Secondly, peaks in Fig. 2 are clearly distinguishable. This is possible only if $t_{sep,C} < t_{eq,C}$, where the separation and equilibration times, $t_{sep,C}$ and $t_{eq,C}$, of complex C are defined as follows:

$$t_{sep,C} = \frac{W}{\Delta v_C} \quad \text{at } C = (DP)^a, (DP)^b, DPP \tag{35}$$

$$t_{eq,C} = \frac{1}{k_C + P_{dep} k_{on,C}} \quad \text{at } C = (DP)^a, DPP \tag{36}$$

$$t_{eq,C} = \frac{1}{k_C + k_{on,C}} \quad \text{at } C = (DP)^b \tag{37}$$

Here, P_{dep} is the depleted concentration of the free protein after applying an electric field and removing the unbound protein from the plug; W is the initial plug length, and Δv_C is the difference

Table 1
Equilibrium and rate constants determined from experimental data and corresponding best fit models shown in Fig. 2.

P (nM)	$C = (DP)^a$			$C = (DP)^b$			$C =$ DPP			P^0 (nM)	D^0 (nM)
	$K_{d,C}$ (nM)	$10^4 k_C$ (s^{-1})	$10^4 k_{on,C}$ ($(nM)^{-1}\,s^{-1}$)	$K_{d,C}$	$10^4 k_C$ (s^{-1})	$10^4 k_{on,C}$ (s^{-1})	$K_{d,C}$ (nM)	$10^4 k_C$ (s^{-1})	$10^4 k_{on,C}$ ($(nM)^{-1}\,s^{-1}$)		
200	132.9	1.2	0.01	8.9	30.0	3.4	543.0	89.1	0.2	116.2	82.6
254	128.8	1.7	0.01	8.8	36.9	4.2	536.3	78.0	0.1	153.7	71.2
424	13.3	2.3	0.2	8.4	39.0	4.6	486.4	59.9	0.1	243.6	7.9
530	1.3	2.5	1.9	6.3	40.0	6.3	130.1	30.0	0.2	285.5	0.6
636	1.3	2.6	2.0	5.4	41.0	7.6	76.8	25.0	0.3	367.4	0.3
848	1.4	2.9	2.0	1.9	64.1	33.7	36.1	21.0	0.6	510.6	0.06

P is the initial (i.e. before the formation of complexes) concentration of *E. coli* SSB protein in the mixtures. The corresponding concentration of a 79-nt long single stranded DNA is 200 nM in all cases. P^0 and D^0 are the equilibrium concentrations of protein and DNA, respectively, in the mixtures.

between velocities of complex C and complex resulting from the dissociation of C (Fig. 1). Condition $t_{sep,C} < t_{eq,C}$ gives $k_C < 10^{-1}\,s^{-1}$, $P_{dep}k_{C,on} < 10^{-1}\,s^{-1}$ at C = $(DP)^a$ (in this case $\Delta v_C = 0.05\,cm\,s^{-1}$) and $k_C < 10^{-2}\,s^{-1}$, $P_{dep}k_{C,on} < 10^{-2}\,s^{-1}$ at C = $(DP)^b$, DPP (in this case $\Delta v_C = (0.003–0.007)\,cm\,s^{-1}$) for a values of $W = 0.5$ cm used in experiments shown in Fig. 2. These inequalities are satisfied (with large margin) by values obtained from the best-fit procedure (Table 1).

Thirdly, dissociation constants, $K_{d,C}$, of complexes C can be estimated directly from experimental data (Fig. 2) using areas, A_C, of corresponding peaks (C = $(DP)^a$, $(DP)^b$, DPP) and relation $P^0 \sim P$

$$K_{d,(DP)^a} \sim \frac{P^0 A_D}{A_{(DP)^a}}, \qquad K_{d,(DP)^b} \sim \frac{A_{(DP)^a}}{A_{(DP)^b}}, \qquad K_{d,DPP} \sim \frac{P^0 A_{(DP)^b}}{A_{DPP}} \tag{38}$$

Such direct estimates also agree with results presented in Table 1.

Finally, fitting the mathematical model into experimental data is possible with small relative errors of 5.6% (Fig. 2). This fact also suggests that the developed theory adequately describes processes of separation and sequential dissociation of DNA complexes with multiple proteins.

According to results shown in Table 1, the equilibrium constants and some of the rate constants appear to depend on SSB concentration. This dependence is especially pronounced for the $(DP)^a$ complex. Such effect can be attributed (at least partially) to the influence of charges of free SSB protein molecules even though

$$\lambda_D \ll l, \quad l \approx (N_A P^0)^{-1/3} \tag{39}$$

Here, λ_D is the Debye length of the buffer ($\lambda_D \sim 10^{-7}$ cm for 25 mM Borax), N_A is Avogadro's number, and l is a characteristic distance between each complex (including free DNA) and the nearest molecules of free SSB protein ($l \sim 10^{-5}$ cm at $P^0 = 500$ nM). Let us consider, for example, a free DNA molecule that binds a protein molecule. Electric charges of almost all other protein molecules (located at distances $\sim$ or $> l$ from this DNA molecule) are screened due to relation (39). Nevertheless, there is always a small probability that other protein molecules are positioned at distances much closer than l, in particular, at distances $\sim r_D$. Of course, such protein molecules account for only a small fraction of all protein molecules. Therefore, they could affect protein binding by only a small fraction of DNA molecules *if the equilibrium concentrations of free DNA and free protein were of the same order of magnitude* ($D^0 \sim P^0$). However, the ratio D^0/P^0 decreases from 0.7 down to 1.2×10^{-4} with an increase in the initial protein concentration P from 200 nM up to 848 nM (Table 1). As a result, even a *small* fraction of protein molecules at $P \geq 424$ nM (i.e. ones that are positioned at distances $\sim r_D$) would be enough to affect protein binding by *almost all* DNA molecules. Similarly, the concentration of $(DP)^b$ decreases to approximately one hundredth of P^0 when P reaches 848 nM. In contrast, the concentration of DPP complex is much smaller than that of free protein at $P = 200$ nM and becomes of the same order of magnitude as P^0 at $P = 848$ nM. Because of that, the influence of free protein molecules on DPP kinetics should vanish at higher protein concentrations. These described effects could lead to a dependence of the rate and equilibrium constants on the initial protein concentration. The presence of charged protein molecules in proximity to each of the following complexes: D, $(DP)^a$, and $(DP)^b$, seems to increase the value of k_{on} for the previous (in sequence (2)) complex, i.e. the value of k_{on} for $(DP)^a$, $(DP)^b$, and DPP, respectively. Similarly, the presence of charged protein molecules in proximity to the $(DP)^b$ and DPP complexes appears to increase values of k for the same complex (for the DPP complex, the last effect occurs at lower initial concentrations of SSB protein). In total, such influence of the charged protein molecules on rate constants results in decreasing values of all $K_{d,C}$ with an increase in the initial protein concentration (Table 1).

Interestingly, rate constants presented in Table 1 are considerably smaller than previously reported values; $k_{on} \sim 1\,(nM)^{-1}\,s^{-1}$ and $k \sim 5 \times 10^{-2}\,s^{-1}$ for the DP complex of SSB protein [37]. Such large rate constants were obtained for oligonucleotide $(dT)_{70}$ by means stopped flow studies. This oligonucleotide consists of 70 identical dT nucleotides, whereas we used a specific 79-mer oligonucleotide composed of all four nucleotides (see Section 3). Experimental conditions (10 mM Tris, pH 8.1) [37] were also different from ours. Obviously, we would not see a separation and multiple peaks in CE experiments at all for $k_{on} \sim 1\,(nM)^{-1}\,s^{-1}$. Experimental data presented in Fig. 2 lead to an inequality $P_{dep}k_{C,on} < 10^{-1}\,s^{-1}$ for C = $(DP)^a$ (as we pointed out earlier in this subsection) and, therefore, to an estimate $k_{C,on} < 10^{-3}\,(nM)^{-1}\,s^{-1}$ even at $P_{dep} = 100$ nM. It is worth noting that a direct measurement of rate constants is impossible and therefore one has to use appropriate mathematical models to calculate rate constants based on signals observed experimentally. Thus, oligonucleotides, experimental methods and conditions and corresponding mathematical models, that resulted in larger rate constants for SSB protein [37], differ significantly from ours. This makes comparison of results a difficult task and we suggest using theoretical arguments for estimation of an upper limit for possible values of k_{on}. Obviously, characteristic binding time $\tau_{on} = (P^0 k_{on})^{-1}$ cannot be smaller than diffusion time τ_{dif} required for the nearest protein molecule to reach a DNA molecule. During this time, a protein molecule has to travel the distance of $\sim l$ if $D^0 \sim P^0$ (in this case, the number of protein molecules positioned at distances much closer than l is negligible in comparison to the number of free DNA molecules). Using the well known expression for diffusion distance corresponding to time τ_{dif} [41,42]:

$$l \approx \sqrt{D_{dif}\tau_{dif}} \tag{40}$$

and the second relation (39) we have

$$\tau_{dif} \approx \frac{l^2}{D_{dif}} \approx \frac{1}{D_{dif}}(N_A P^0)^{-2/3}, \quad \tau_{dif} \approx 10^{-3}\,s \;\; \text{at} \;\; P^0 = 100\,nM \tag{41}$$

Here D_{dif} is the diffusion coefficient of protein molecules ($D_{dif} \sim 5 \times 10^{-7}\,cm^2\,s^{-1}$). If each collision between protein and DNA molecules resulted in formation of the $(DP)^a$ complex, characteristic binding time would be the same order of magnitude as diffusion time ($\tau_{on} \sim \tau_{dif}$). Maybe such a situation is possible under specific physiological conditions, if nucleotides exhibit some cooperative binding effect. However, we should have $\tau_{on} \gg \tau_{dif}$ in a general case when they lose such ability. Indeed, the crystallographic structure of the complex between a 28-nt long ssDNA and SSB protein (PDB code 1EYG) shows that this DNA positions itself on the surface of SSB protein tetramer in a specific conformation, with the oligonucleotide center being in close proximity to the K62 binding residue [35]. The total solvent accessible area of all four K62 residues in the tetramer accounts for a small fraction ($\sim 10^{-2}$) of the solvent accessible area of the tetramer as it is evident from its structure (PDB code 1QVC) [36]. Actually, this fraction should be even smaller since SSB protein in the structure was truncated to 145 residues from 177 residues of the native *E. coli* SSB protein. Thus, the probability of binding (without cooperativity of nucleotides), during a collision between the 28-mer oligonucleotide and the SSB protein tetramer, can be estimated as less than $10^{-2}C_{conf}{}^{-1}$, where C_{conf} is the number of possible conformations of the oligonucleotide on the tetramer surface. Of course, longer oligonucleotides can be bound to the K62 residue at any point in their central section but they will also have a larger number of conformations, C_{conf}. Obviously, $C_{conf} \gg 1$, though it is difficult to estimate this number more precisely. As a result, the characteristic binding time should be significantly greater than

the diffusion time ($\tau_{on} \sim$ or $> 10^2 C_{conf} \tau_{dif}$). Finally, we can write the following estimation for k_{on}

$$k_{on} = \frac{1}{P^0 \tau_{on}} \leq \frac{1}{10^2 C_{conf} P^0 \tau_{dif}} \quad (42)$$

For example, at $C_{conf} = 10^3$ and $P^0 = 100$ nM (given $\tau_{dif} \approx 10^{-3}$ s), we have an estimate of $k_{on} \sim$ or $< 10^{-4}$ (nM)$^{-1}$ s^{-1} that agrees with the results presented in Table 1.

3. Materials and methods

3.1. Preparation of protein–DNA complexes

We produced complexes of SSB protein and a 79-nt long single stranded DNA. SSB proteins bind to single-stranded DNA with high affinity and are important in DNA functions [32–34,40]. A fluorescently labeled 79-mer oligonucleotide 5-FAM/CTC CTC TGA CTG TAA CCA CGA GAA ATT GGT ACT GTA TGA AAC GGC AGC TGC ACG TCG CGG CAT AGG TAG TCC AGA AGC C (IDT Technologies, Coralville, IA, USA) was mixed with the SSB protein. Six mixtures were prepared (with DNA to protein ratios of approximately 1:1, 1:1.3, 1:2.1, 1:2.6, 1:3.2, and 1:4.2) in which the DNA concentration was 200 nM and the SSB protein concentrations were 200 nM, 254 nM, 424 nM, 530 nM, 636 nM, and 848 nM (before the formation of complexes). The mixtures were incubated for sufficiently long time so that further incubation did not influence the results. All buffer components were from Sigma–Aldrich (Oakville, ON). All aqueous solutions were made with deionized water and filtered through a 0.22-μm filter (Millipore, Nepean, ON). SSB protein was purchased from Interscience (Markham, ON, Canada). The protein and DNA stock solutions as well as equilibrium mixtures were prepared in the incubation buffer (25 mM Borax, pH 10).

3.2. Capillary electrophoresis

A short plug of the equilibrated mixture was then injected into the capillary by pressure and a high voltage CE run was performed to separate the SSB protein and the DNA–protein complexes with different velocities. A single-point detector was used to record cumulative electropherograms. CE experiments were performed with a CE instrument (P/ACE MDQ, Beckman-Coulter, USA) with thermo-stabilization of the capillary (the outer walls of the capillary were washed with a liquid heat exchanger maintained at 15 °C) and sample vials were kept at 15 °C. The instrument employed laser-induced fluorescence detection with a 488 nm line of an argon-ion laser for fluorescence excitation. An uncoated fused silica capillary (Polymicro, Phoenix, AZ) with a 20-μm inner diameter and a length of 50 cm was used. The length L from the injection end to the detection window was 40 cm. Electrophoresis was run with a positive electrode at the injection end and an electric field E of 600 V cm^{-1}. The run buffer was identical to the incubation one. The length W of sample plugs was 0.55 cm.

4. Concluding remarks

In this work we considered the kinetics of the sequential dissociation of DNA–multiple protein complexes in a separation based approach. All complexes, unbound proteins and DNA move with different velocities and the free protein is quickly removed from the mixture (Fig. 1a). As a result, the formation of complexes due to association with free protein is negligible in comparison to the dissociation of the complexes (Fig. 1b). We found exact analytical solutions (11), (18), and (21) of the mass transfer equations (3) and (4). The latter describe the processes of migration and sequential dissociation in the general case of N complexes, where N is an arbitrary integer. These analytical solutions allow one to calculate concentrations (5) of complexes and their cumulative signal (6) at any point x and moment t. For the first three stages in the sequential dissociation of complexes, the complex concentrations were presented in a simplified form (26)–(33). Theoretical results were tested with data obtained for three-stage dissociation of DNA complexes with SSB protein. Calculated signals were in a good agreement with the experimentally measured ones (Fig. 2). Analytical solutions describing sequential dissociation of complexes moving with different velocities can be used in numerical simulations of experiments and in studies of dissociation kinetics using a separation based approach.

Acknowledgment

This work was funded by the Natural Sciences and Engineering Research Council of Canada.

References

[1] B. Schrofelbauer, Y. Hakata, N.R. Landau, Proc. Natl. Acad. Sci. U.S.A. 104 (2007) 4130–4135.
[2] L. Saiz, J.M.G. Vilar, IET Syst. Biol. 2 (2008) 247–255.
[3] M. Verma, S. Rawool, P.J. Bhat, K.V. Venkatesh, Biosystems 84 (2006) 39–48.
[4] E. Margeat, A. Bourdoncle, R. Margueron, N. Poujol, V.V. Cavailles, C. Royer, J. Mol. Biol. 326 (2003) 77–92.
[5] V. Pavski, X.C. Le, Curr. Opin. Biotechnol. 14 (2003) 65–73.
[6] J.J.-C. Lin, S.E. Grosskurth, S.M. Harlan, E.A. Gustafson-Wagner, Q. Wang, Methods Mol. Biol. 366 (2007) 183–201.
[7] W.D. Wilson, Science 295 (2002) 2103–2105.
[8] R.B.M. Schasfoort, A.J. Tudos, Handbook of Surface Plasmon Resonance, RSC Pub., Cambridge, UK, 2008.
[9] P.L. Privalov, A.I. Dragan, Biophys. Chem. 126 (2007) 16–24.
[10] J.T. Gerstle, M.G. Fried, Electrophoresis 14 (1993) 725–731.
[11] J. Vistica, J. Dam, A. Balbo, E. Yikilmaz, R.A. Mariuzza, T.A. Rouault, P. Schuck, Anal. Biochem. 326 (2004) 234–256.
[12] G.J. Howlett, A.P. Minton, G. Rivas, Curr. Opin. Chem. Biol. 10 (2006) 430–436.
[13] D.B. Green, J. Lane, R. Wing, Appl. Spectrosc. 41 (1987) 847–851.
[14] M.D. Christianson, C.R. Landis, Concepts Magn. Reson., Part A 30A (2007) 165–183.
[15] N. Fang, D.D.Y. Chen, Anal. Chem. 77 (2005) 840–847.
[16] N.H.H. Heegaard, C. Schou, J. Østergaard, J. Methods Mol. Biol. 421 (2007) 303–338.
[17] Y. Sun, N. Fang, D.D.Y. Chen, Electrophoresis 29 (2008) 3333–3341.
[18] X. Liu, F. Dahdouh, M. Salgado, F.A. Gomez, J. Pharm. Sci. 98 (2009) 394–410.
[19] P.N. Zaikin, E.V. Khoroshilova, Comput. Math. Model. 6 (1995) 96.
[20] M. Lupu, D. Todor, Chemom. Intell. Lab. Syst. 29 (1995) 11–17.
[21] S.N. Krylov, Biomol. Screen. 11 (2006) 115–122.
[22] V. Okhonin, S.M. Krylova, S.N. Krylov, Anal. Chem. 76 (2004) 1507–1512.
[23] A. Petrov, V. Okhonin, M. Berezovski, S.N. Krylov, J. Am. Chem. Soc. 127 (2005) 17104–17110.
[24] V. Okhonin, A.P. Petrov, M. Berezovski, S.N. Krylov, Anal. Chem. 78 (2006) 4803–4810.
[25] R. Bharadwaj, C.C. Park, L. Kazakova, H. Xu, J.S. Paschkewitz, Anal. Chem. 80 (2008) 129–134.
[26] H.L. Wang, T. Li, Anal. Chem. 81 (2009) 1988–1995.
[27] P. Yang, Y. Mao, A.W.-M. Lee, R.T. Kennedy, Electrophoresis 30 (2009) 457–464.
[28] E.J. Carrasco-Correa, M. Beneito-Cambra, J.M. Herrero-Martinez, G. Ramis-Ramos, J. Chromatogr. A 1218 (2011) 2334–2341.
[29] A.P. Petrov, L.T. Cherney, B. Dodgson, V. Okhonin, S.N. Krylov, J. Am. Chem. Soc. 133 (2011) 12486–12492.
[30] W.J. Wiscombe, J.W. Evans, J. Comput. Phys. 24 (1977) 416–444.
[31] P. De Groen, B. De Moor, J. Comput. Appl. Math. 20 (1987) 175–187.
[32] I.J. Molineux, S. Friedman, M.L. Gefter, J. Biol. Chem. 249 (1974) 6090–6098.
[33] M.M. Cox, I.R. Lehman, J. Biol. Chem. 257 (1982) 8523–8532.
[34] T.M. Lohman, M.E. Ferrari, Annu. Rev. Biochem. 63 (1994) 527–570.
[35] S. Raghunathan, A.G. Kozlov, T.M. Lohman, G. Waksman, Nat. Struct. Biol. 7 (2000) 648–652.
[36] T. Matsumoto, Y. Morimoto, N. Shibata, T. Kinebuchi, N. Shimamoto, T. Tsukihara, N. Yasuoka, J. Biochem. (Tokyo) 127 (2000) 329–335.
[37] A.G. Kozlov, T.M. Lohman, Biochemistry 41 (2002) 6032–6044.
[38] S.V. Kuznetsov, A.G. Kozlov, T.M. Lohman, A. Ansari, J. Mol. Biol. 359 (2006) 55–65.
[39] R. Roy, A.G. Kozlov, T.M. Lohman, T. Ha, J. Mol. Biol. 369 (2007) 1244–1257.
[40] M. Ryzhikov, O. Koroleva, D. Postnov, A. Tran, S. Korolev, Nucleic Acids Res. 39 (2011) 6305–6314.
[41] A. Einstein, Investigations on the Theory of Brownian Movement, Dover Publications, 1956, 119 p.
[42] B.H. Lavenda, Nonequilibrium Statistical Thermodynamics, John Wiley & Sons Inc., 1985, 214 p.